

# The estimation of the hardly reducible background in a system of IACTs

Dorota Sobczyńska\*

\*University of Łódź, Department of Astrophysics, Pomorska 149/153, 90-236 Łódź, Poland

**Abstract.** The IACT (Imaging air Cherenkov telescope) measure images of the showers initiated by cosmic ray particles. Differences between the image shape of the proton and  $\gamma$  induced showers make the preliminary selection of the primary  $\gamma$  possible, while the analysis of the image direction is the final step of the  $\gamma$ /hadron separation. The detection of the hadronic images, which contain the Cherenkov light from one electromagnetic subcascade in the shower, is possible for a large area detectors. This kind of detected events are hardly reducible by using the parameters describing the image shape only. Also the images made by Cherenkov photons from two electromagnetic subcascades, which are products of the same  $\pi^0$  decay, should look similar to that originated by primary photon. The fraction of both kind of images (made by one or two correlated subcascades) in the protonic background has been estimated by Monte Carlo simulations for the system of two MAGIC-like telescopes. The SIZE ranges which are mostly affected by such background are shown. The ratio of the expected number events of such background to the number of the triggered high energy photons from the Crab direction was estimated for a small  $\theta^2$  parameter.

**Keywords:** VHE  $\gamma$ -astronomy, IACT's,  $\gamma$ /hadron separation

## I. INTRODUCTION

In IACTs experiments the number of events induced by this hadronic background is several orders of magnitude larger than the number of the registered  $\gamma$ -rays from the source. The  $\gamma$ /hadron separation method based on the Hillas parameter [1] is commonly used for a measurement with a single telescope and a system of telescopes. Telescopes with a very large area (CANGAROO [2], [3], HESS [4], [5], MAGIC [6], [7], VERITAS [8], [9]) have been built in order to measure a low energy primary photons. In the low energy region the difficulties with the  $\gamma$ /hadron separation are caused by higher relative fluctuations in the shower development, which results in larger fluctuations of the Cherenkov light density [10], [11] and image parameters. Additionally the Earth's Magnetic Field influences on the image parameters [12] more at low than at high energy primary  $\gamma$ -rays events.

There is a special kind of background - images containing a light from a single charge particle in protonic shower. The possible rejection of such events have been studied in [13], [14].

Images of one electromagnetic subcascade from hadron-initiated showers were found as a hardly reducible background [15], [16], [17]. Those events were called *false  $\gamma$  images* in [16], [17] and I will call them the same in this paper. The image may contain photons from only two  $\gamma$  subcascades, which originated from the same particle. I shall call them *one  $\pi^0$  images*.

One of the only two physical reasons for differences in shapes of the false and the true  $\gamma$ -ray images is the different height of the first  $e^+$ ,  $e^-$  pair production. The false  $\gamma$  events start deeper in the atmosphere (in the average) and by that a narrower angular distribution of the charged particles is expected. Due to that fact their images may be narrower than those of real  $\gamma$ -ray events. Slightly wider images may be expect in the case of one  $\pi^0$  events due to the existence of the separation angle between the decay products. The second possibly reason of differences between the shape of true and false  $\gamma$  images is the direction of both cascades (fixed and extended for true and false  $\gamma$  events respectively).

The major image axis of the hadronic background is distributed randomly and false  $\gamma$  and one  $\pi^0$  images should have the same features in spite to the true primary photons, which major axis should be directed towards the source direction on the camera plane. One can expect that the parameter which is describing the orientation of the image is still a good quantity for the true  $\gamma$ -ray selection.

All results presented in this paper are based on a Monte Carlo simulation for two Cherenkov telescopes similar to the MAGIC II experiment [18]. In the following I present the MC study and estimate the fraction of false  $\gamma$  and one  $\pi^0$  events in the proton showers. The distribution of the parameters describing the image shape are presented to show the similarity of true and false  $\gamma$  events. The ratio of the expected number of both false  $\gamma$  and one  $\pi^0$  images to that of primary  $\gamma$ -rays from the Crab Nebula direction is calculated in different SIZE bins and for different trigger thresholds. This ratio is shown also for events surviving simple mean scaled WIDTH and LENGTH cuts. The occurrence of false  $\gamma$  and one  $\pi^0$  events is an important reason for the low efficiency of the  $\gamma$ /hadron separation in the low SIZE range of the stereo IACTs.

## II. MONTE CARLO SIMULATIONS

The shower development in the atmosphere was simulated using the CORSIKA code [19], [20]. MAGIC II [18] was chosen as an example of a stereo system of

IACTs. The system contains two 17m diameter telescopes. The distance between them is 85 m. In the simulations presented in this paper the second telescope is exactly the same as the first one (more technical details are given in [21], [6], [22]).  $25 \cdot 10^6$  showers initiated by primary protons with energies between 30 GeV and 1 TeV with a differential spectral index of -2.75 were simulated. The impact parameter was distributed randomly within a circle (radius of 1.2 km) around the center of the telescopes system. The showers were simulated within a cone with an opening angle of  $5.5^\circ$  at a zenith angle of  $20^\circ$  and an azimuth of  $0^\circ$  (showers directed to the north).

The  $\gamma$  cascade were simulated with the impact parameter, which was randomly distributed within a circle of 350 m radius. The energy range of 10 GeV to 1 TeV has been chosen. The differential spectral index was chosen to be -2.6 (which is the index of the Crab spectrum for energies above 300 GeV [23] or 500 GeV [24]). The direction of  $0.5 \cdot 10^6$  simulated  $\gamma$  cascades was fixed to a zenith angle of  $20^\circ$  and an azimuth angle of  $0^\circ$  (parallel to the axes of both telescopes).

Additional information about each subcascade that has been produced in the EAS was kept in the modified CORSIKA code (more details in [16], [17]). Rayleigh and Mie scattering of light in the atmosphere were taken into account [25].

The night sky background (NSB) which was measured on La Palma [26], was included in the simulation before checking the trigger conditions. Photoelectrons made by the NSB were not added to the images to avoid the necessity of the so called cleaning procedure. One may expect that an image cleaning with too high cleaning levels may make images artificially narrower. A comparison of the image parameters after cleaning may be by that less reliable.

The simulations were done for two telescopes working in a stereo system. A single telescope was triggered by a shower if the output signals in three next neighbouring pixels (3 NN) exceed a certain threshold. The trigger thresholds have been chosen to be: 2, 3, 4, 5 in arbitrary units (hereafter referred to as *a.u.* or *p.e.* in the legend of figure 6), which corresponds to the signal of 2, 3, 4 and 5 photoelectrons (p.e.) arriving exactly at the same time [27], respectively.

### III. RESULTS AND DISCUSSION

The impact parameter distribution of the proton induced shower is shown in figure 1 for trigger threshold 2 a.u. All triggered, electromagnetic, one  $\pi^0$  and false  $\gamma$  events are presented as different histograms. It can be seen that the range of the simulated impact parameter is large enough to cover the interesting area on the ground (the slopes of all distributions are similar at large impact parameter). The one  $\pi^0$  and false  $\gamma$  events have quite flat distributions between 100 and 600 m and 300 and 700m respectively. Figure 2 shows the distribution of the angular distance between the telescope axis and

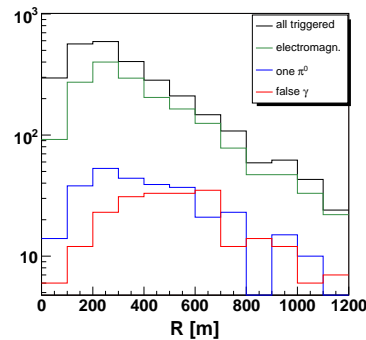


Fig. 1. The impact parameter distribution of the proton initiated showers for trigger threshold 2 a.u.

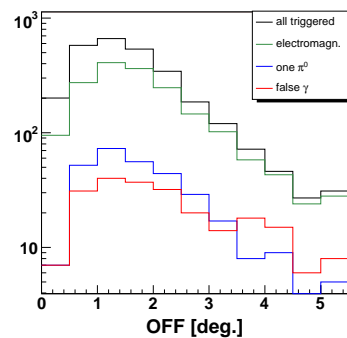


Fig. 2. The distribution of angular distance between the telescope axis and shower axes; trigger threshold 2 a.u.

the shower axis (so called OFF) for proton showers. It can be seen that also the simulation range of the OFF parameter was sufficient.

Figure 3 shows the primary energy distribution of the triggered proton events, for a trigger threshold of 2 a.u. The distributions for both one  $\pi^0$  and false  $\gamma$  events are much steeper than that of all triggered events for primary energies above 100 GeV. Similar results have been shown in [16] for a single telescope and a different trigger condition. Most of the one  $\pi^0$  and false  $\gamma$  events have a primary energy below 250 GeV.

One may estimate the expected number of triggered events for energies above 1 TeV (assuming the probability of the triggering an event, that has an impact parameter larger than 1200 m or OFF parameter larger than  $5.5^\circ$  is negligible in comparison to all triggered showers). In order to do that a simple power law fit of the energy distribution tail was used as an extrapolation function. Similar estimations were done for both one  $\pi^0$  and false  $\gamma$  events in order to calculate the fraction of images imitating true  $\gamma$ -ray events in the expected protonic background. The contribution of both false  $\gamma$  and one  $\pi^0$  images in all triggered events decreases from 25% to 9% when the trigger threshold increases from 2 a.u. to 5 a.u. The numbers presented here have been obtained from the number of events which images which contain up to 10 % of light from other particles from the shower.

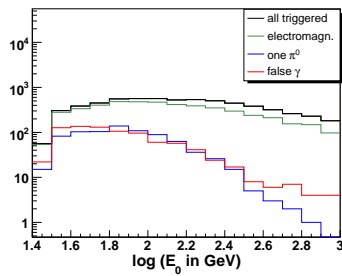


Fig. 3. The energy distribution for primary proton (trigger threshold 2 a.u.)

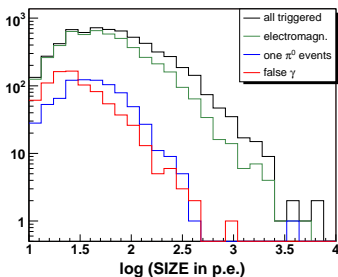


Fig. 4. SIZE distributions - proton images (trigger threshold 2 a.u.).

The SIZE distribution of images registered by one of the telescopes is shown in figure 4. Both false  $\gamma$  events and one  $\pi^0$  images have small SIZES because their primary energy is relatively low and they may have quite large impact parameter, where the expected SIZE is low.

The fraction of both false  $\gamma$  and one  $\pi^0$  events in the total number of triggered proton showers depends on the chosen SIZE interval. This fraction is higher for small SIZES than for large SIZES. The reconstructed energy of  $\gamma$  candidates is proportional to the SIZE and thus one can expect more events of the hardly reducible background in low the low energy.

Figure 5a shows a distribution of the mean scaled WIDTH [28] for the simulated  $\gamma$ -ray and both false  $\gamma$  and one  $\pi^0$  images (the trigger thresholds 3 a.u.). All histograms are normalized to 1. The WIDTH distributions are very similar. It has been check that large value of the mean scaled WIDTH are caused by one  $\pi^0$  events, where wider angular distribution of charged particle is expected due to the existence of the separation angle between the decay products.

The distributions of the mean scaled LENGTH for primary  $\gamma$ -rays and both false  $\gamma$  and one  $\pi^0$  events are presented in figure 5b. False  $\gamma$  and one  $\pi^0$  events are inclined to the telescope's axes and thus a longer part of the shower may be visible to the detector. This results in a larger image LENGTH. It has been checked that in the low OFF range the distributions are more similar. The second reason for larger mean scaled LENGTH is the existence of the separation angle of the decay products.

The expected number of both false  $\gamma$  and one  $\pi^0$  images with  $\theta^2 < 0.02^\circ^2$  was estimated using the primary proton spectrum[29], [30]. The background

from primary He has been added assuming that they produce the same fraction of hardly reducible background as primary protons. The Crab spectrum measured by MAGIC in 2005 [23] was used to calculate the expected number of real  $\gamma$  events. The spectrum was extrapolated to energies below 300 GeV. New measurements of the spectrum show that it is flatter below 300 GeV [31] thus the expected number of true  $\gamma$ -rays can be overestimated.

The ratio of both false  $\gamma$  and one  $\pi^0$  images to that of primary  $\gamma$ -rays from the Crab Nebula direction has been calculated in different SIZE bins. Figure 6a shows the result for trigger thresholds 2, 3, 4 and 5 a.u., respectively (no  $\gamma$ /hadron separation method was applied to this plot). Figure 7b presents the same ratio as figure 7a but calculated after a simple  $\gamma$ -ray selection. Cuts in the mean scaled WIDTH and LENGTH have been applied (both between -2.0 and 0.5). Any false  $\gamma$  and one  $\pi^0$  events with SIZE larger than 250 p.e. has been found after those cuts in the simulated Monte Carlo data-set. The similarity of true and false  $\gamma$  image shapes results in a significant reduction of the  $\gamma$ /hadron separation efficiency in the low SIZE range. This is one of the main reasons why the sensitivity of IACTs is worsening in the low energy range.

#### IV. CONCLUSIONS

Two large Cherenkov telescopes working in stereo mode may be triggered by photons from one electromagnetic subcascade or from one  $\pi^0$  subshowers of proton-induced showers. This kind of background is mostly caused by low energy proton induced showers. The distance between the center of the telescope system and the shower axis position may be very large. No specific range of the inclination angle of the shower to the telescopes axes has been found.

The proton background contains around 25% of false  $\gamma$  or one  $\pi^0$  events at a trigger threshold of 2 a.u which decreases to 9% at a trigger threshold of 5 a.u. The fraction of false  $\gamma$  images in the proton background stongly depends on the investigated SIZE range. This fraction is much higher for lower SIZES than for higher SIZES.

The images of the false and true  $\gamma$ -ray have similar shapes - the differences in the WIDTH and LENGTH distributions are mostly caused by different shower direction distributions and the existence of the separation angle between the decay products.

The efficient true  $\gamma$ -ray selection from one  $\pi^0$  and false  $\gamma$  images is not possible by using only the shape parameters in a single MAGIC-like telescope [16]. The results presented in this paper show that similar problem appears in a system of two large IACTs. However the ratio of the expected background from false  $\gamma$  and one  $\pi^0$  events to the number of the triggered high energy photons from the direction of the Crab Nebula is a few times lower for a stereo measurement than for a single telescope detection [16] in the same SIZE range. This fact may be explain by a more precise estimation of the

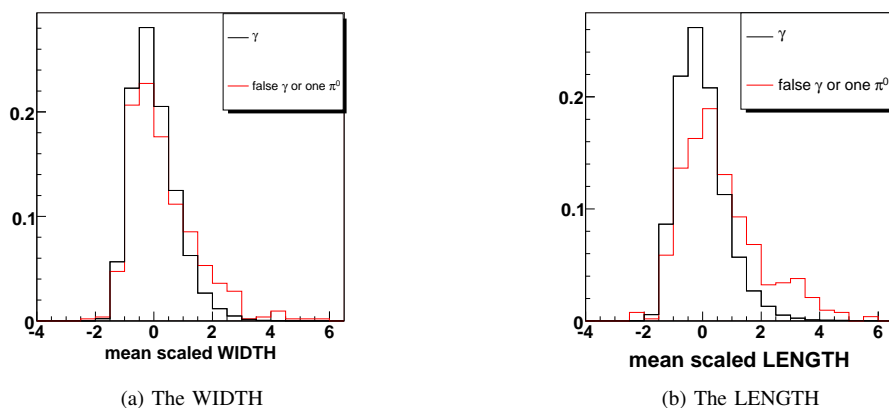


Fig. 5. Distributions of the mean scaled WIDTH and the mean scaled LENGTH. All histograms are normalised to 1. The comparison between true  $\gamma$ -rays and both false  $\gamma$  and one  $\pi^0$  events (trigger threshold 3 a.u.).

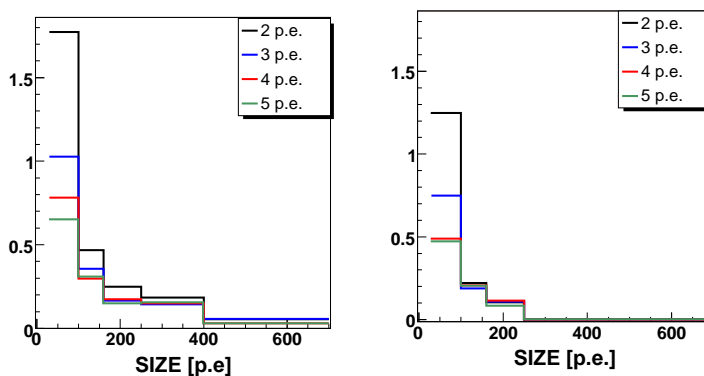


Fig. 6. Ratio of the expected number of false  $\gamma$  and one  $\pi^0$  images to the expected number of true  $\gamma$ -rays (from the direction of the Crab Nebula) in different SIZE bins for  $\theta^2$  smaller than 0.02: **a)** before mean scaled WIDTH and LENGTH cuts; **b)** after simple mean scaled WIDTH and LENGTH cuts (see text).

shower direction for two IACTs.

The false  $\gamma$  and one  $\pi^0$  events survive a simple selection based on the image shape parameters in the low SIZES range. In conclusion the sensitivity of a stereo system of IACTs is worsening at lower energies because of the existence of a hardly reducible background: false  $\gamma$  and one  $\pi^0$  events.

#### REFERENCES

- [1] Hillas A M 1985 *Proc. 19th Int. Cosmic Ray Conf. (La Jolla)* vol 3, p 445 (1985)
- [2] Enomoto R *et al* 2002 *Astropart. Phys.* **16** 235
- [3] Mori M *et al* 2005 *Proc. Towards a Network of Atmospheric Cherenkov Detectors VII Conf. (Palaiseau)* p 19
- [4] Vasileiadis G *et al* 2005 *Nucl. Instrum. Methods Phys. Res. A* **553** 268
- [5] Hofmann D *et al* 2005 *Proc. Towards a Network of Atmospheric Cherenkov Detectors VII Conf. (Palaiseau)* p 43
- [6] Baixeras C *et al* 2004 *Nucl. Instrum. Methods Phys. Res. A* **518** 188
- [7] Mariotti M *et al* 2005 *Proc. Towards a Network of Atmospheric Cherenkov Detectors VII Conf. (Palaiseau)* p 29
- [8] Weekes T C *et al* 2002 *Astropart. Phys.* **17** 221
- [9] Weekes T C *et al* 2005 *Proc. Towards a Network of Atmospheric Cherenkov Detectors VII Conf. (Palaiseau)* p 3
- [10] Chitnis V R and Bhat P N 1998 *Astropart. Phys.* **9** 45
- [11] Sobczynska D 2009 *J.Phys.G: Nucl. Part. Phys.* **36** 045201
- [12] Commichau *et al* 2008 *Nucl.Instrum. Methods Phys. Res. A* **592** 572
- [13] Mirzoyan R *et al* 2006 *Astropart. Phys.* **25** 342
- [14] Aliu E *et al* 2009 *Astropart. Phys.* **30** 293
- [15] Maier G and Knapp J. 2007 *Astropart. Phys.* **28** 72
- [16] Sobczynska D 2007 *J.Phys.G: Nucl. Part. Phys.* **34** 2279
- [17] Sobczynska D 2009 *submitted to J.Phys.G: Nucl. Part. Phys.*
- [18] Carmona E *et al* 2007 *Proc. 30th Int. Cosmic Ray Conf. (Merida, Mexico)* vol 3 1373
- [19] Heck D *et al* 1998 Technical Report FZKA 6019 (Forschungszentrum Karlsruhe)
- [20] Knapp J and Heck D 2004 EAS Simulation with CORSIKA: A Users Manual
- [21] Barrio J A *et al* 1998 The MAGIC Telescope Design Study (Munich)
- [22] Albert J *et al* 2005 *Astropart Phys* **23** 493
- [23] Wagner R *et al* 2005 *Proc. 29th Int. Cosmic Ray Conf. (Pune)* vol 4 163
- [24] Aharonian F *et al* 2004 *Astrophys. J.* **314** 897
- [25] Sokolsky P 1989 "Introduction to Ultrahigh Energy Cosmic Ray Physics" Addison-Wesley
- [26] Mirzoyan R and Lorenz E 1994 MPI-PhE/94-35 preprint (Munich)
- [27] Sobczyńska D and Lorenz E 2002 *Nucl. Instrum. Methods Phys. Res. A* **490** 124
- [28] Aharonian F *et al* 2006 *Astron.and Astrophys* **457** 899
- [29] Haino S *et al* 2004 *Phys. Lett. B* **594** 35
- [30] Hareyama M and Shibata T 2005 *Int. J. Modern Phys. A* **29** 6769
- [31] Albert J *et al* 2008 *Astrophys. J.* **674** 1037